Elsevier Editorial System(tm) for Deep-Sea Research Part II
Manuscript Draft

Manuscript Number:

Title: Circulation, stratification and seamounts in the South West Indian Ocean

Article Type: SW Indian Ocean Ridge

Keywords: ocean circulation
subtropical gyre
mesoscale eddies
seamounts
Agulhas Current
Southwest Indian Ocean (20-45°S, 25-60°E)

Corresponding Author: Prof. Raymond Trevor Pollard, PhD

Corresponding Author's Institution: National Oceanography Centre

First Author: Raymond Trevor Pollard, PhD

Order of Authors: Raymond Trevor Pollard, PhD; Jane F Read

Circulation, stratification and seamounts in the South West Indian Ocean

Raymond Pollard[1] and Jane Read[1]

[1]National Oceanography Centre
University of Southampton Waterfront Campus
European Way
Southampton SO14 3ZH
United Kingdom

Corresponding author: raymond.pollard@gmail.com
telephone: +44 1590682118

Abstract

Circulation in the vicinity of six seamounts along the Southwest Indian Ridge was studied as part of a multidisciplinary survey in November 2009. Examination of altimetric data shows that several of the seamounts lie in the area of slow mean westward flow between the southern tip of Madagascar (25°S) and the Agulhas Return Current (ARC) flowing eastward between 37-40°S. The mean westward drift of mesoscale features was 4.1 ± 0.9 cm s^{-1}. Integrated between Madagascar and 37°S, this westward drift can account for 50 Sv (1 Sv = $10^6 m^3 s^{-1}$), which, added to 25 Sv of southward flow past Madagascar, is sufficient to account for the total Agulhas Current transport of 70 ± 21 Sv. The transport of the ARC was also measured, at two longitudes, down to 2000 m. Combined with earlier crossings of the ARC in 1986 and 1995, the full depth transport of the ARC is estimated at 71 – 85 Sv at longitudes 40 – 50°E, indicating that the Agulhas Current then ARC transport continues unreduced as far as 50°E before beginning to recirculate in the Southwest Indian Ocean subtropical gyre. The primary control on the circulation near each seamount was its position relative to any mesoscale eddy at the time of the survey. Melville lay on the flank of a cyclonic eddy that had broken off the ARC and was propagating west before remerging with the next meander of the ARC. Nearby Sapmer, on the other hand, was in the centre of an anticyclonic eddy, resulting in very weak stratification over the seamount at the time of the survey. Middle of What lies most often on the northern flank of the ARC, in strong currents, but was at the time of the survey near the edge of the same eddy as Sapmer. Coral, in the Subtropical Front south of the ARC, was in waters much colder, fresher, denser and more oxygenated than all the other seamounts. Walter was close to the path of eddies propagating southwest from east of Madagascar, while Atlantis, the furthest east and north seamount, experienced the weakest eddy currents.

Keywords

Ocean circulation subtropical gyre; mesoscale eddies; seamounts;

Agulhas Return Current; Southwest Indian Ocean (20 – 45°S, 25 – 60°E)

1. Introduction

In late 2009, the research vessel *Dr. Fridtjof Nansen* carried out a 6-week multi-disciplinary survey of six seamounts in the Southwest Indian Ocean (**Fig. 1**). The purpose of this paper is to summarize the mean circulation and the role of mesoscale eddies in modifying the circulation and stratification at each seamount at the time of the cruise.

Six seamounts were surveyed (**Table 1**), five of which lay along the line of the Southwest Indian Ridge (Fig. 1), which is split by deep fracture zones. Atlantis, Melville and Coral seamounts were situated on ridges just east of the Atlantis, Indomed and Discovery II Fracture Zones respectively; Sapmer was just west of the Gallieni Fracture Zone; Middle of What (MoW) was a deeper feature on the ridge between Melville and Sapmer. Walter was another deep feature situated on the west side of the Madagascar Ridge, and northwest of the Walter's Shoals, the shallowest part of the Ridge.

A limited number of physical oceanographic observations were made at each seamount, including a short CTD section and a 24-hour CTD yoyo. A few CTD stations were also occupied on passage and two CTD sections across the Agulhas Return Current (ARC)

were worked. Shipboard acoustic Doppler current profiler (ADCP) data were acquired throughout the cruise. Shipboard data have been supplemented with Maps of Absolute Dynamic Topography (MADT) (**Fig. 2**), obtained from the SSALTO/DUACS (Segment Sol multimissions d'ALTimétrie, d'Orbitographie et de localisation precise/Developing Use of Altimetry for Climate Studies) multimission altimeter data processing system, distributed by CLS/AVISO (Collecte Localis Satellites/Archivage, Validation, Interprétation des données des Satellite Océanographiques). Fig. 2a shows the synoptic surface circulation on 18 November 2009, when the first seamount, Atlantis, was being surveyed. Four weeks later (Fig. 2b), the survey of the final seamount, Walter, had just ended.

The best known current in the Southwest Indian Ocean is the Agulhas Current (Lutjeharms, 2006), running to the southwest down the east coast of South Africa (Fig. 2). To the south of Africa, the Agulhas Current retroflects to the east, meandering between 37°S and 41°S in the Agulhas Return Current (ARC). The ARC weakens to the east as transport peels off to the north (Lutjeharms, 2007; Stramma and Lutjeharms, 1997) to close the anticyclonic (anticlockwise) Southwest Indian Ocean Subtropical Gyre.

South of the ARC, two areas of closely spaced sea surface height (SSH) contours can be identified (Fig. 2), marking the Subtropical Front (STF) (Belkin and Gordon, 1996; Read *et al.*, 2000) and the Subantarctic Front (SAF). The SAF is marked by the tightening of SSH contours just east of Coral (Fig. 2, transition from green to yellow), and is the northern edge of the Antarctic Circumpolar Current (ACC), which reaches it northernmost circumpolar excursion at 50°E (Pollard and Read, 2001; Pollard *et al.*, 2007). Thus Coral seamount lies just north of the ACC but in the path of the STF and, on occasion, the ARC (Boebel *et al.*, 2003).

2. Eastward transport along the southern boundary of the Subtropical Gyre

Two closely spaced hydrographic sections (Fig. 2), between Coral and Melville (33 km station spacing) and south of MoW (28 km spacing), allow us to identify the ARC, STF and SAF and estimate their boundaries and separate eastward transports. Using temperature and salinity range criteria for these fronts at several depths (Belkin and Gordon, 1996) and the 300 – 800 m depth range for the 10°C isotherm to identify the ARC (Belkin and Gordon, 1996), we have identified the CTDs nearest to the boundaries between the ARC, STF and SAF and overlaid them on the sea surface height contours of Fig. 2b (**Fig. 3**). The bold dashed lines in Fig. 3 connect these CTDs following sea surface height contours. There are only small offsets between the estimated frontal boundaries and the sea surface height contours on each section, so our choice of frontal boundaries is consistent between the two sections.

Geostrophic transports for adjacent station pairs (Fig. 3) have been calculated down to 1500 m relative to 1500 m for comparison with other estimates (Lutjeharms and Ansorge, 2001). Note the transport minimum between the ARC and STF on each section (2.9 and 3.0 Sv on west and east sections respectively), which indicates a separation between the ARC and STF transports. However, there is no minimum between STF and the SAF (seen only on the eastern section) so we cannot reliably apportion the transport between the two.

Transports for the ARC are 44 and 51 Sv for the 45°E and 50°E sections (Fig. 3). The difference between these estimates could have several explanations. The anticyclonic eddy around Sapmer and the large gap between MoW and the next station to the south could have increased the transport for the eastern section. Transports could have changed during the week that elapsed between the occupations of the two sections. For comparison, the transport of the Agulhas Current was observed to change from its minimum 9 Sv to its maximum 122 Sv in only 24 days (Bryden *et al.*, 2005) so changes of over 4 Sv per day are observed. Our ARC transports are consistent with previous estimates. For *RRS Discovery* cruise 164 (Read and Pollard, 1993) in 1986 the equivalent (above 1500 m) ARC transport across 40°E was 49 Sv (calculated as 42 Sv by (Lutjeharms and Ansorge, 2001). For *Discovery* cruise 213 (Pollard and Read, 2001) in 1995 the ARC transport across 41°E was 44 Sv. Thus all four sections give estimates of ARC transport in the range 44 – 51 Sv across 40-50°E.

The cruise 164 and 213 *Discovery* sections allow us to scale up the 1-1500 m *Nansen* transports to full depth transports because all CTDs were full depth. The full depth ARC transports for cruises 164 and 213 were respectively 84.2 Sv (Read and Pollard, 1993) and 71.3 Sv (Pollard and Read, 2001) and the ratios of 1500 m transport to full depth transport are 0.57 and 0.62, average 0.6. Scaling up by 1.67, the *Nansen* estimates of full depth transport are 73.0 Sv at 45°E and 84.7 Sv at 50°E, in close agreement with the previous measurements (71.3 Sv at 42 – 43°E and 84.2 Sv at 41 – 42°E). In summary, we have 4 estimates of full depth ARC transport: 84, 71, 73 and 85 Sv at 41, 42, 45 and 50°E respectively, which closely match two published estimates of the Agulhas Current transport, 73 Sv (Beal and Bryden, 1999) and 85 Sv (Toole and Warren, 1993). Bryden *et al.* (2005), by creating a time series of Agulhas Current transport from moorings that also resolve the Agulhas Undercurrent (Beal and Bryden, 1999), have revised these estimates downwards to 70 ± 21 Sv.

We conclude that the data sets discussed here suggest that the Agulhas Current then ARC transport continues unreduced as far as 50°E. Thus significant leakage from the ARC back into the Southwest Indian Ocean subtropical gyre does not begin until east of 50°E. This differs somewhat from previous work (Lutjeharms and Ansorge, 2001). Transferring the northern boundary of the ARC marked on Fig. 3 onto Fig. 2b and extending it along the relevant sea surface height contour (~100 cm, Fig. 2) suggests that northward return flow lies primarily east of Sapmer (say 55°E). There is also some leakage from the cyclonic eddies that regularly break off north from the ARC.

For the STF we can do similar calculations. Cruises 164 and 213 yielded STF transports down to 1500 m of 10.5 and 12.5 Sv, 0.53 and 0.89 of the full depth transports 19.8 and 14.1 Sv. These compare with 9.6 and 14.5 Sv for the *Nansen* sections. However, the 14.5 Sv is rather large, and likely includes a contribution from SAF transport, which cannot be separated. Thus our best estimates of the STF full depth transports remains 14 – 20 Sv from the *Discovery* sections.

Our estimate of 9.8 Sv for the SAF transport at 50°E is a minimum, likely enhanced by a contribution from the adjacent STF. At 50°E the SAF is at its northernmost extent at any longitude (Pollard *et al.*, 2007), and there is further transport which has bypassed the meander observed by our short transect and which rejoins further east (Fig. 2b).

3. Closure of the Subtropical Gyre, westward transport

How the closure of the Subtropical Gyre is achieved is still a subject of active research (Lutjeharms, 2007). There are three main sources for the Agulhas Current, southward flow between Mozambique and Madagascar, southwestward flow east of Madagascar and westward flow between Madagascar and the ARC. Recent research (de Ruijter *et al.*, 2004; de Ruijter *et al.*, 2005) has shown that the first two sources comprise eddies and dipoles that contribute about 25 Sv (Lutjeharms, 2007; Stramma and Lutjeharms, 1997) to the Agulhas transport. Examples are apparent in Fig. 2. Arrows on Fig. 2a mark the paths of a number of eddies that have been tracked from weekly AVISO images for three months, ending on 18 November 2009, the date of the Fig. 2a image. Focus on the two anticyclonic eddies just south of Madagascar along 28°S. The eddy at 45°E had formed and drifted southwestward at 10.7 cm s^{-1} over three months, then continued southwestward at 15.2 cm s^{-1} (Fig. 2b) during the 4-week period between Fig. 2a and Fig. 2b, appearing to form a dipole (de Ruijter *et al.*, 2004) with the cyclonic eddy just west of it. The eddy at 41°E had drifted westwards at a mean speed of 6.9 cm s^{-1} over 3 months (Fig. 2a) and continued west at 12.1 cm s^{-1} for the next 4 weeks (Fig. 2b) in a dipole with the cyclonic eddy just north of it. This dipole pair appears to merge with the Agulhas a week or two after Fig. 2b. The southwestward tracking eddy, on the other hand, appears to slow down and weaken over the weeks after Fig. 2b, but then drifts west to lose its momentum to the Agulhas.

The third Agulhas source, westward flow between Madagascar and the ARC, is the least studied and the largest, estimated to be 35-40 Sv down to 1000 m (Lutjeharms, 2007). A movie of the weekly AVISO images from 2009 up to March 2010 (from which Fig. 2 is drawn), shows clear westward propagation of eddies (see Fig. 2 for examples), which can also be seen in Hovmöller diagrams (Boebel *et al.*, 2003; Quartly *et al.*, 2006; Schouten *et al.*, 2002) extracted from the AVISO images (**Fig. 4**). It is now well established that the westward propagating features are eddies rather than Rossby waves (Chelton *et al.*, 2011), and we shall show that their propagation speeds are in any case larger than can be attributed to Rossby waves (Killworth *et al.*, 1997). At latitudes 27-33°S westward propagation is apparent at all longitudes. At 35°S and 37°S the westward propagation stalls west of about 35°E, countered by the influence of the Agulhas and ARC.

The longitude v. time slope of over 60 features has been measured (**Table 2**) to examine their westward speeds and whether there are variations with time, latitude or longitude. Splitting the features into two time periods, the first and second halves of the 15 months plotted in Fig. 4, showed no significant temporal differences, so both time periods have been merged in Table 2. Westward propagation speeds are similar at all latitudes except 27°S (Table 2), where they are significantly larger. At 27°S, eddies heading west after rounding the southern tip of Madagascar (as discussed above) lead to larger westward propagation speeds (12.5 cm s^{-1}) than further south (7.1 cm s^{-1}). Table 2 also shows significantly larger propagation speeds west of 45°E than east of 45°E at all latitudes. This divergence is consistent with input of water from the north, from east of Madagascar, enhancing westward flow.

To estimate the strength of inflow from the east, excluding any northern influence, we therefore restrict ourselves to features south of 27°S and east of 45°E. Table 2 shows consistent feature propagation of 4.1 ± 0.9 cm s^{-1} over 40 observations, the standard

deviation of the mean being only 0.1 cm s^{-1}. It is interesting to note that, if we integrate the westward speed of 4.1 cm s^{-1} down to 1000m (Lutjeharms, 2007) south from Madagascar to 37°S, the transport would sum to 50 Sv, exceeding Lutjeharm's estimate of 35-40 Sv. Thus the mean westward flow is indeed sufficient to close the transport budget of the Agulhas Current.

Between 37°S and 40°S the westward drift interacts with the intense, eastward flowing ARC. The large meanders of the ARC (Boebel *et al.*, 2003) spawn cyclonic eddies to the north of the ARC which propagate west along 37.5°S at an average speed of 5.4 cm s^{-1} (Boebel *et al.*, 2003) until reabsorbed into the next meander trough to the west. Boebel *et al.* found that such eddies were shed nearly exclusively in austral fall (March-May), but the dashed lines around Melville on Fig. 2a show the path of such an eddy which was spawned in early July 2009 and reabsorbed about 6 months later. Another cyclonic eddy southeast of Sapmer can be seen moving west and being reabsorbed in Fig. 2b.

In summary, we have shown that eastward transport by the ARC can account for all the transport of the Agulhas Current of 70 Sv (Bryden *et al.*, 2005) as far east as 50°E. East of 50°E, transport begins to peel off to the north to close the gyre circulation. These results update and modify previous conclusions (Lutjeharms and Ansorge, 2001). At all latitudes between the ARC and the southern tip of Madagascar, there is evidence for westward drift of eddies at an estimated speed of 4.1 cm s^{-1}, which suggests a westward transport of as much as 50 Sv, which is sufficient to account for the Agulhas Current transport when added to southward flow of 25 Sv east and west of Madagascar (de Ruijter *et al.*, 2005) and is more than Lutjeharms' estimate of 35-40 Sv of westward flow (Lutjeharms, 2007).

4. Circulation near seamounts

We end with an overview of how the mean circulation and mesoscale eddies affect the physical structure at each seamount, using both AVISO and *in situ* data. The circulation at each seamount is determined more by its proximity to an eddy than by the weak mean flow, and eddies and their propagation can be determined from Fig. 2. Features in weekly AVISO sea surface height data from July to December 2009 are described. Longer term information on ARC influence at each seamount has been obtained by processing the weekly AVISO images for three years, from 7 January 2009 up to 7 December 2011. For each image, the sea surface height and derived east and north surface velocities have been extracted, at grid points close to each seamount, from the mapped, updated product, yielding 153 week time series at each seamount. The statistics of these time series (**Table 3**) give an indication of how often each seamount is affected by the ARC. For *in situ* data, we have derived mean profiles at each seamount (**Fig. 5**) by averaging the 24-hour yoyo CTDs at each site.

Coral was the only seamount of the survey that was situated south of the ARC and STF but north of the SAF, in the Subantarctic Zone (Pollard *et al.*, 2002) with correspondingly low temperatures and salinities, high oxygens and densities. Between 50 and 100 m stratification was controlled by salinity, with a marked halocline at mean depths between 70 and 100 m, and a fresh surface layer. From July 2009 up to the cruise occupation in early December Coral was always in or on the southern side of the STF. Thus eastward circulation of about 10-20 cm s^{-1} prevailed. Over three years, the mean surface speed at

Coral was 21 cm s^{-1} but reached a maximum of 83 cm s^{-1} proving ARC influence. Speeds over 40 cm s^{-1} occurred about 10% of the time, when anticyclonic meanders of the ARC penetrated south.

In July 2009, Melville was located on the northern edge of ARC, at the northern tip of a developing meander that broke off as a cyclonic eddy in August. The eddy (whose path is shown dashed on Fig. 2a) moved a small distance north then west (Fig. 2a) such that Melville lay on its western then southern then eastern edge. By November, the meander that spawned the eddy had moved east until it was south of MoW (Fig. 2). In early January 2010 the eddy remerged with the next westward meander of the ARC to the one which spawned it (Boebel *et al.*, 2003). When the site was occupied in December, altimeter derived velocities were approximately 20 cm s^{-1} to the southwest (Fig. 2b). Melville is the closest seamount to the core of the ARC, so shows the highest mean (34 cm s^{-1}) and maximum (94 cm s^{-1}) speeds and variability over three years (Table 3). Speeds were greater than 40 cm s^{-1} over 30% of the time.

MoW most often lies on the northern flank of the ARC, and did so for several months after mid-December 2009 (Fig. 2b). In October and November 2009, however, MoW lay near the edge of an anticyclonic eddy that formed in August between two northward meanders of the ARC, then moved slowly to the northwest from October. During the survey, MoW lay on the south side of the elongated centre of the eddy (Fig. 2b), in southeast to east currents of up to 30 cm s^{-1}. MoW lies about as far north of the core of the ARC as Coral lies south, so shows similar statistics (Table 3), being affected by northward penetrating cyclonic meanders of the ARC, which resulted in speeds of 40 cm s^{-1} being exceeded 16% of the time.

The anticyclonic eddy which influenced MoW in late 2009 also affected Sapmer (on its northwest flank) from early September 2009, being centred on Sapmer in mid-November (Fig. 2a), and continued to affect Sapmer, on its southeast flank, until late January 2010. Thus, when Sapmer was occupied on 22 - 24 November (Table 1), the presence of the eddy resulted in remarkably weak stratification (Fig. 5c) down to over 400 m (i.e. below the crest of the seamount). Note the relatively high oxygens down to 400 m at Sapmer, hinting at deep mixing from the surface. The sea surface height at Sapmer during the cruise (nearly 130 cm, Fig. 2b) was the highest over three years, showing that the eddy was the strongest, but there were six sea surface height maxima in that period, of which two reached 120 cm, so that mesoscale eddies regularly affect that site. However, Sapmer is too far north to be directly influenced by the ARC, with surface current speeds always less than 40 cm s^{-1}.

Atlantis and Walter seamounts are both several degrees north of the other seamounts, hence have greater near-surface stratification (Fig. 5c). Atlantis sees a slow westward drift of weak, mostly cyclonic eddies. During the cruise, a weak anticyclone to the southeast of Atlantis gave rise to small (<20cm s^{-1}) currents at the surface in a west to southwesterly direction. Walter, on the other hand, was situated just to the southeast of the track of rapidly translating eddies from east of Madagascar. One of these anticyclonic eddies of light, tropical water lay to the north and a second, slow-moving cyclonic eddy of denser, subtropical water had moved to the south of Walter by the time it was surveyed (Fig. 2b). Hence flow past the seamount was to the east averaging 20 cm s^{-1}. Over three years, Walter shows slightly higher current statistics than Atlantis, because it is regularly

affected by the eddies propagating south from East of Madagascar. Oxygens are particularly low at Walter as a result of the southward flow of low-oxygen water.

Comparing properties at the six seamounts (Fig. 5), all but Coral have near-identical water masses in the thermocline (Fig. 5f), but isopycnals in the thermocline (say 26.4 kg m^{-3}, Fig. 5c) are shallowest at Coral and Atlantis, the southern and northeast corners of the survey respectively. This reflects the strong eastward flow of the ARC north of Coral, but more interestingly, confirms the westward drift between Atlantis and the seamounts near the ARC. Oxygen values (Fig. 5d) at all but two seamounts increase towards the surface, indicating that the spring bloom and summer stratification have not taken hold. At Atlantis and Walter the decrease in oxygen above 50 m matches the strong near-surface stratification (Fig. 5c). Fluorescence at all seamounts, although uncalibrated, was very low, but in all cases there was a subsurface peak, close to 100 m deep at Atlantis and Walter, shallower at all other seamounts.

5. Conclusions

We have shown that the Agulhas Current transport can all be accounted for in the Agulhas Return Current, flowing eastwards to 50°E, with large meanders, between 37°S and 41°S. This transport, 71 – 85 Sv, results in surface currents up to about 100 cm s^{-1} within the core of the ARC. The subtropical front carries a further 14 – 20 Sv. Three of the six seamounts surveyed, Coral, Melville and MoW, are strongly influenced by the ARC, experiencing surface currents of over 40 cm s^{-1} during 10%, 30% and 16% of a three year period, respectively. These currents occur either when the seamount is in the core of the ARC or in mesoscale eddies that regularly spin off the ARC.

North of the ARC a large number of mesoscale eddies are observed, in general propagating westwards at mean speeds of 4.1± 0.9 cm s^{-1}. From this westward drift, a westward transport of up to 50 Sv has been estimated, which, together with 25 Sv of southward transport east and west of Madagascar (Lutjeharms, 2007), accounts for the 70 ± 21 Sv Agulhas transport (Beal and Bryden, 1999). All the seamounts surveyed are influenced by eddies on occasion, resulting in mean currents past a seamount of up to 30 – 50 cm s^{-1}.

Stratification in the upper 400 m varied considerably between the six seamounts. It was largest at Walter and Atlantis, the northernmost sites, and weakest at Sapmer, because Sapmer was in the centre of a deep-extending anticyclonic eddy when it was surveyed.

Acknowledgements

The authors would like to thank the officers, crew and scientists of the RV Dr Fridtjof Nansen cruise 2009 410 without whose help these data would not have been collected. This work was supported by the NERC large scale observing programme.

330 **Tables**

331 **Table 1 – Seamounts surveyed**

Seamount	**Atlantis**	**Sapmer**	**Middle of What**	**Coral**	**Melville**	**W of Walters Shoal**
Latitude °S	32.6-32.9	36.7-37.0	37.8-38.1	41.3-41.6	38.3-38.6	31.5-31.8
Longitude °E	57.1-57.5	51.9-52.3	50.2-50.6	42.7-43.1	46.5-46.9	42.65-43.05
Minimum depth	750 m (70m min)	350 m	1100m	200 m	100 m	1250 m
depth of CTD yoyo	700 m	500 m	900 m	400 m	500 m	1200 m
dates occupied	17-19Nov	22-24Nov	25-27Nov	2-4Dec	7-10Dec	12-13Dec
jdays occupied	321-323	326-328	329-331	336-338	341-344	346-347

332

333

334

335 **Table 2 – Westward speeds of eddy propagation**

	Features west of 45°E			Features east of 45°E		
Latitude °S	Mean cm/s	Standard deviation	Number in sample	Mean cm/s	Standard deviation	Number in sample
27	12.5	0.8	2	7.3	1.7	4
29	7.8	1.2	5	4.2	1.3	7
31	8.4	1.5	6	4.2	1.1	6
33	7.1	0.4	3	4.3	0.6	8
35	5.7	1.7	5	4.3	0.8	10
37	5.5	0.6	2	3.7	0.7	9
29-37	7.1	1.7	21	4.1	0.9	40

336

337 **Table 3 – Statistics of surface speeds (cm $^{s-1}$) near each seamount**

seamount	Mean speed	Standard deviation	Maximum speed
Atlantis	12	6	27
Sapmer	15	9	39
MoW	23	17	85
Coral	21	15	83
Melville	34	22	93
Walter	18	9	50

338

339

Figures

Fig. 1 The positions of the six seamounts surveyed during the Nansen cruise are shown relative to the bathymetry of the Southwest Indian Ocean and a streamline of the Agulhas Return Current (dashed, see Fig. 2). Five of the seamounts – Atlantis, Sapmer, Middle of What (MoW), Melville and Coral lay along the SouthWest Indian Ridge (SWIR) and Walter was on the west side of the Madagascar Ridge. Sapmer, MoW, Melville and Coral all lay close to the path of the Agulhas Return Current.

Fig. 2 AVISO sea surface height (SSH) maps are shown for (a) 18 Nov (b) 16 Dec 2009, four weeks apart and close to the start (17 Nov, Atlantis) and end (13 Dec, Walter) of the survey. Arrows show the paths of eddies tracked with weekly SSH maps. Numbers are speeds in cm/sec. In (a), arrows show distance travelled in 91 days (3 months) from 19 Aug to 18 Nov. In (b), arrows show the distance travelled by the same features in the 4-week period from 18 Nov to 16 Dec. Dashed lines in (a) show path of cyclonic eddy that broke off ARC from when it was spawned around 8 July to when it coallesced back onto another meander around 20 Jan 2010 after 6 months. Crosses mark CTD and seamount positions. Agulhas Return Current (ARC), SubTropical Front (STF) and SubAntarctic Front (SAF) are marked.

Fig. 3 Heavy dashes mark the boundaries of the Agulhas Return Current (ARC), Subtropical Front (STF) and SubAntarctic Front (SAF) as determined from salinity, temperature and depth range criteria (Belkin and Gordon, 1996) along the two closely spaced CTD sections. Between the sections, the dashed lines are superimposed on sea surface height streamlines from satellite altimetry closest in time to our occupation of the sections (Fig. 2b). Eastward transport (Sv) is annotated for each station pair and summed for each front.

Fig. 4 Hovmöller plots of AVISO sea surface height against longitude and time show westward propagation of features at all latitudes between Madagascar and the ARC. Westward propagation ceases only close to the Agulhas and in the vicinity of the Agulhas retroflection.

Fig. 5 Profiles of (a) potential temperature, (b) salinity, (c) density, (d) oxygen, (e) fluorescence against depth and (f) potential temperature against salinity at each seamount, averaged over 24 hours. Averages of properties including depth were calculated on density surfaces then plotted against the averaged depth, in order to avoid smoothing of features which can result from normal depth averaging. The most pronounced differences were at Coral (blue) where the depth averaged profiles are shown dashed for comparison. Depth averaging is more reliable near the surface and bottom of each profiles. Oxygen and fluorescence are not absolutely calibrated, for lack of calibration data, but depth dependent features are of interest. Subtropical Surface Water (STSW) and Subantarctic Surface Water (SASW) are marked on (f).

References

Beal, L.M., Bryden, H.L., 1999. The velocity and vorticity structure of the Agulhas Current at 32°S. Journal of Geophysical Research 104 (C3), 5151-5176.

Belkin, I.M., Gordon, A.L., 1996. Southern Ocean fronts from the Greenwich Meridian to Tasmania. Journal of Geophysical Research 101 (C2), 3675-3696.

Boebel, O., Rossby, T., Lutjeharms, J., Zenk, W., Barron, C., 2003. Path and variability of the Agulhas Return Current. Deep Sea Research Part II: Topical Studies in Oceanography 50 (1), 35-56.

Bryden, H.L., Beal, L.M., Duncan, L.M., 2005. Structure and transport of the Agulhas Current and its temporal variability. Journal of Oceanography 61 (3), 479-492.

Chelton, D.B., Schlax, M.G., Samelson, R.M., 2011. Global observations of nonlinear mesoscale eddies. Progress in Oceanography 91 (2), 167-216.

de Ruijter, W.P.M., Aken, H.M.v., Beier, E.J., Lutjeharms, J.R.E., Matano, R.P., Schouten, M.W., 2004. Eddies and dipoles around South Madagascar: formation, pathways and large-scale impact. Deep Sea Research Part I: Oceanographic Research Papers 51 (3), 383-400.

de Ruijter, W.P.M., Ridderinkhof, H., Schouten, M.W., 2005. Variability of the southwest Indian Ocean. Philosophical Transactions of the Royal Society A: Mathematical, Physical and Engineering Sciences 363 (1826), 63-76.

Killworth, P.D., Chelton, D.B., de Szoeke, R.A., 1997. The Speed of Observed and Theoretical Long Extratropical Planetary Waves. Journal of Physical Oceanography 27 (9), 1946-1966.

Lutjeharms, J.R.E., 2006. The Agulhas Current. Springer, Berlin.

Lutjeharms, J.R.E., 2007. Three decades of research on the greater Agulhas Current. Ocean Science 3, 129-147.

Lutjeharms, J.R.E., Ansorge, I.J., 2001. The Agulhas Return Current. Journal of Marine Systems 30 (1-2), 115-138.

Pollard, R.T., Lucas, M.I., Read, J.F., 2002. Physical controls on biogeochemical zonation in the Southern Ocean. Deep-Sea Research II 49 (16), 3289-3305.

Pollard, R.T., Read, J.F., 2001. Circulation pathways and transports of the Southern Ocean in the vicinity of the Southwest Indian Ridge. Journal of Geophysical Research 106 (C2), 2881-2898.

Pollard, R.T., Venables, H.J., Read, J.F., Allen, J.T., 2007. Large scale circulation around the Crozet Plateau controls an annual phytoplankton bloom in the Crozet Basin. Deep-Sea Research II 54 (18-20), 1915-1929, doi:1910.1016/j.dsr1912.2007.1906.1012.

Quartly, G.D., Buck, J.J.H., Srokosz, M.A., Coward, A.C., 2006. Eddies around Madagascar -- The retroflection re-considered. Journal of Marine Systems 63 (3-4), 115-129.

Read, J.F., Lucas, M.I., Holley, S.E., Pollard, R.T., 2000. Phytoplankton, nutrients and hydrography in the frontal zone between the Southwest Indian subtropical gyre and the Southern Ocean. Deep-Sea Research I 47 (12), 2341-2367.

Read, J.F., Pollard, R.T., 1993. Structure and transport of the Antarctic Circumpolar Current and Agulhas Return Current at 40°E. Journal of Geophysical Research 98 (C7), 12281-12295.

Schouten, M.W., de Ruijter, W.P.M., van Leeuwen, P.J., 2002. Upstream control of Agulhas Ring shedding. Journal of Geophysical Research 107 (C8), 3109.

Stramma, L., Lutjeharms, J.R.E., 1997. The flow field of the subtropical gyre of the South Indian Ocean. Journal of Geophysical Research 102 (C3), 5513-5530.

Toole, J.M., Warren, B.A., 1993. A hydrographic section across the subtropical South Indian Ocean. Deep-Sea Research 40 (10), 1973-2019.

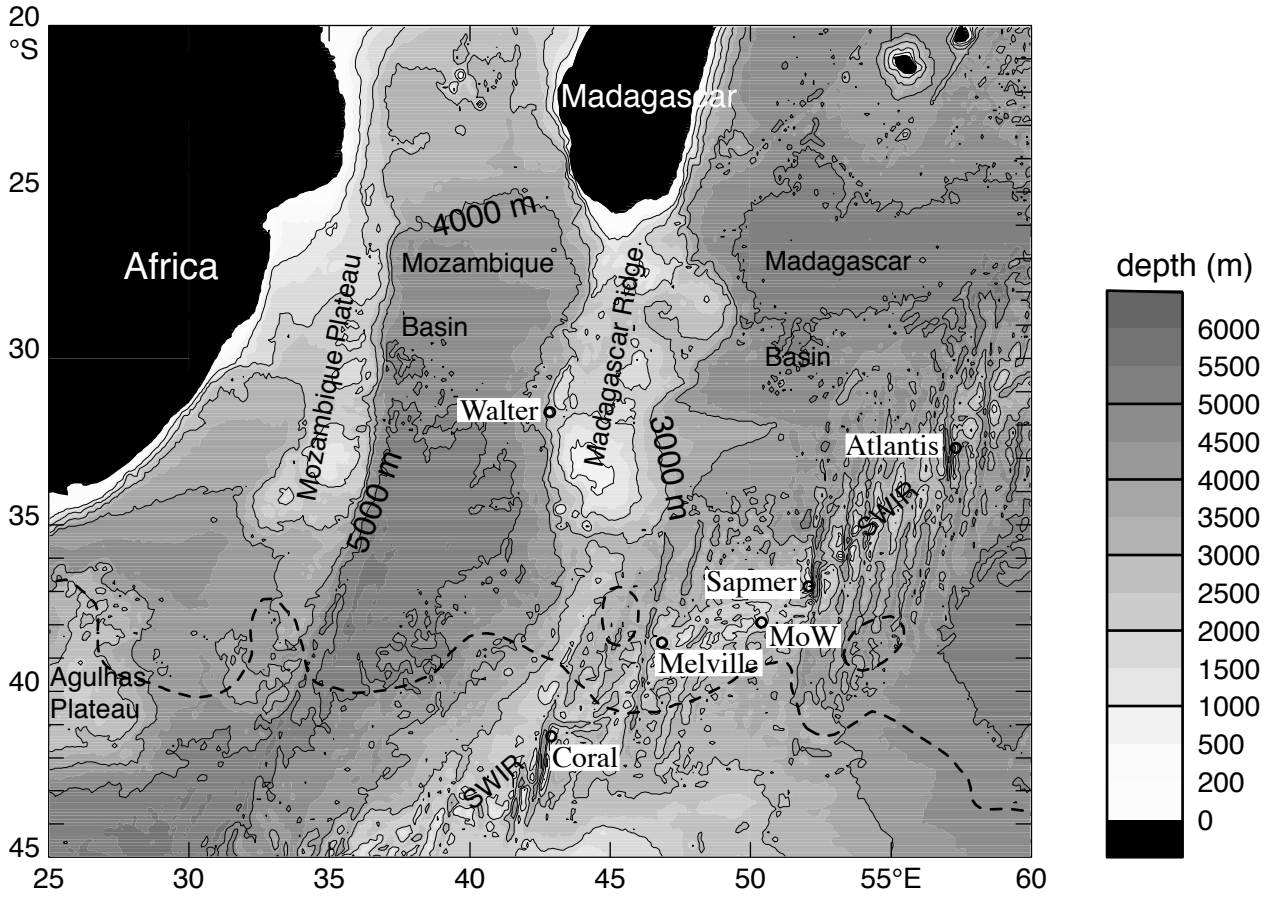

Fig. 1 The positions of the six seamounts surveyed during the Nansen cruise are shown relative to the bathymetry of the Southwest Indian Ocean and a streamline of the Agulhas Return Current (dashed, see Fig. 2). Five of the seamounts – Atlantis, Sapmer, Middle of What (MoW), Melville and Coral lay along the SouthWest Indian Ridge (SWIR) and Walter was on the west side of the Madagascar Ridge. Sapmer, MoW, Melville and Coral all lay close to the path of the Agulhas Return Current.

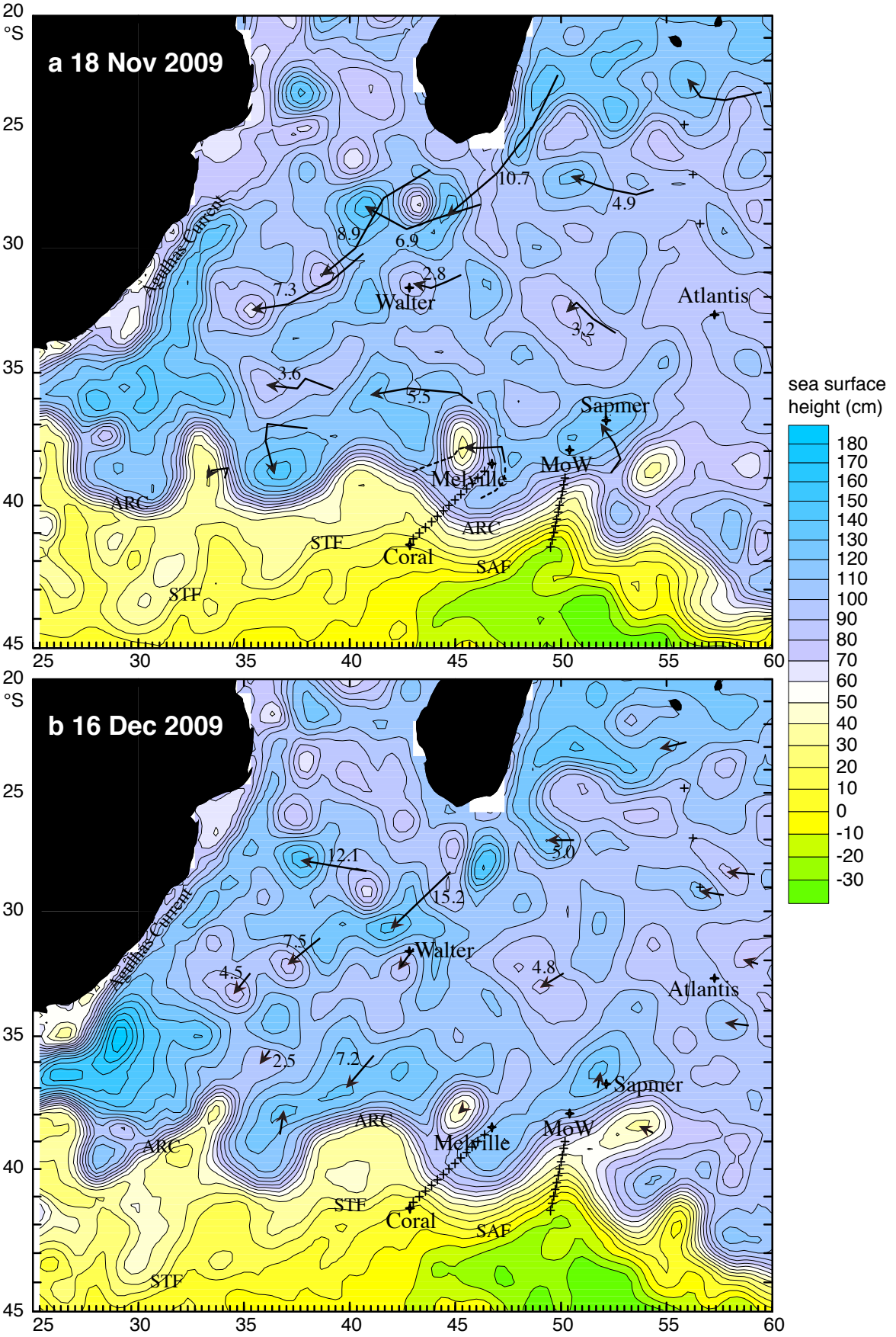

Fig. 2 AVISO sea surface height (SSH) maps are shown for (a) 18 Nov (b) 16 Dec 2009, four weeks apart and close to the start (17 Nov, Atlantis) and end (13 Dec, Walter Shoals) of the survey. Arrows show the paths of eddies tracked with weekly SSH maps. Numbers are speeds in cm/sec. In (a), arrows show distance travelled in 91 days (3 months) from 19 Aug to 18 Nov. In (b), arrows show the distance travelled by the same features in the 4-week period from 18 Nov to 16 Dec. Dashed lines in (a) show path of cyclonic eddy that broke off ARC from when it was spawned around 8 July to when it coallesced back onto another meander around 20 Jan 2010 after 6 months. Crosses mark CTD and seamount positions. Agulhas Return Current (ARC), SubTropical Front (STF) and SubAntarctic Front (SAF) are marked.

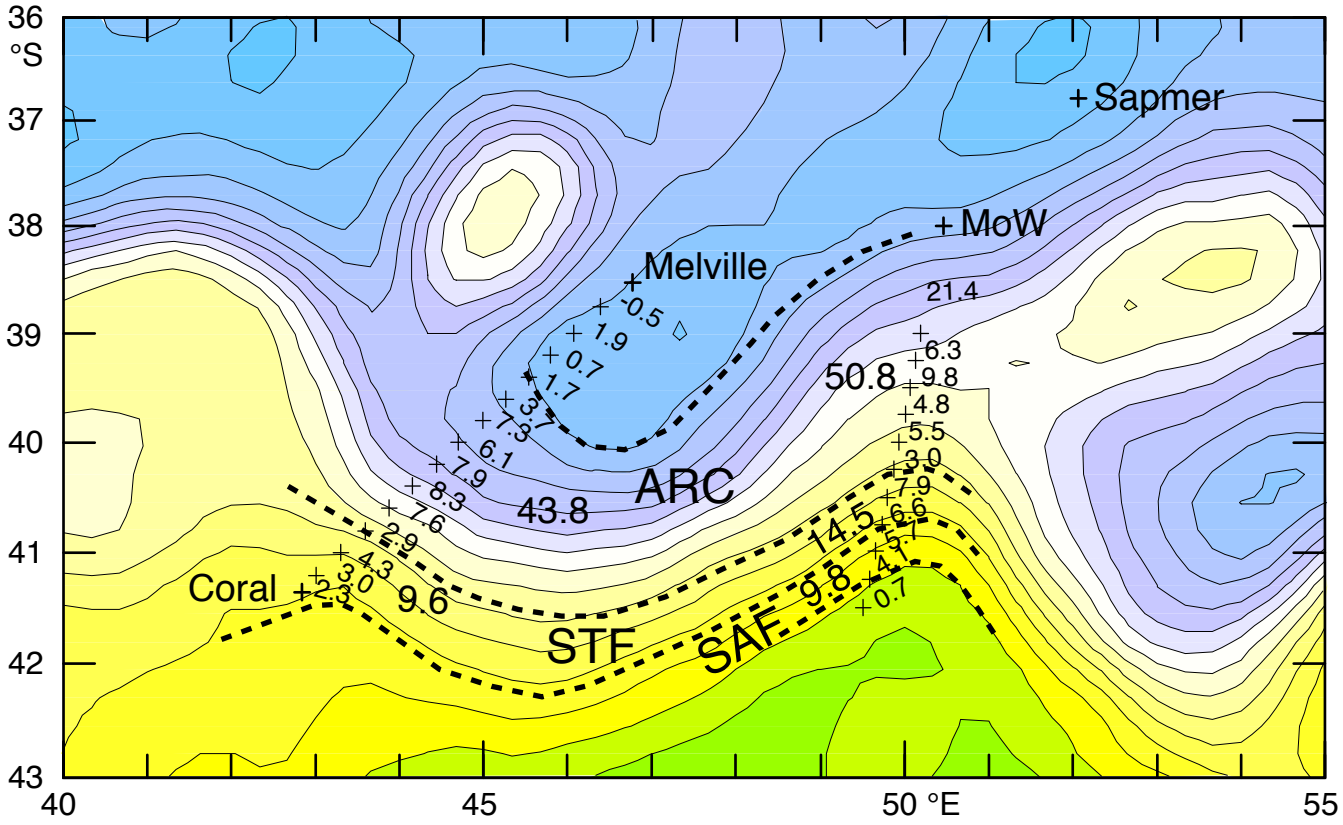

Fig. 3 Heavy dashes mark the boundaries of the Agulhas Return Current (ARC), Subtropical Front (STF) and SubAntarctic Front (SAF) as determined from salinity, temperature and depth range criteria (Belkin and Gordon, 1996) along the two closely spaced CTD sections. Between the sections, the dashed lines are superimposed on sea surface height streamlines from satellite altimetry closest in time to our occupation of the sections (Fig. 2b). Eastward transport (Sv) is annotated for each station pair and summed for each front.

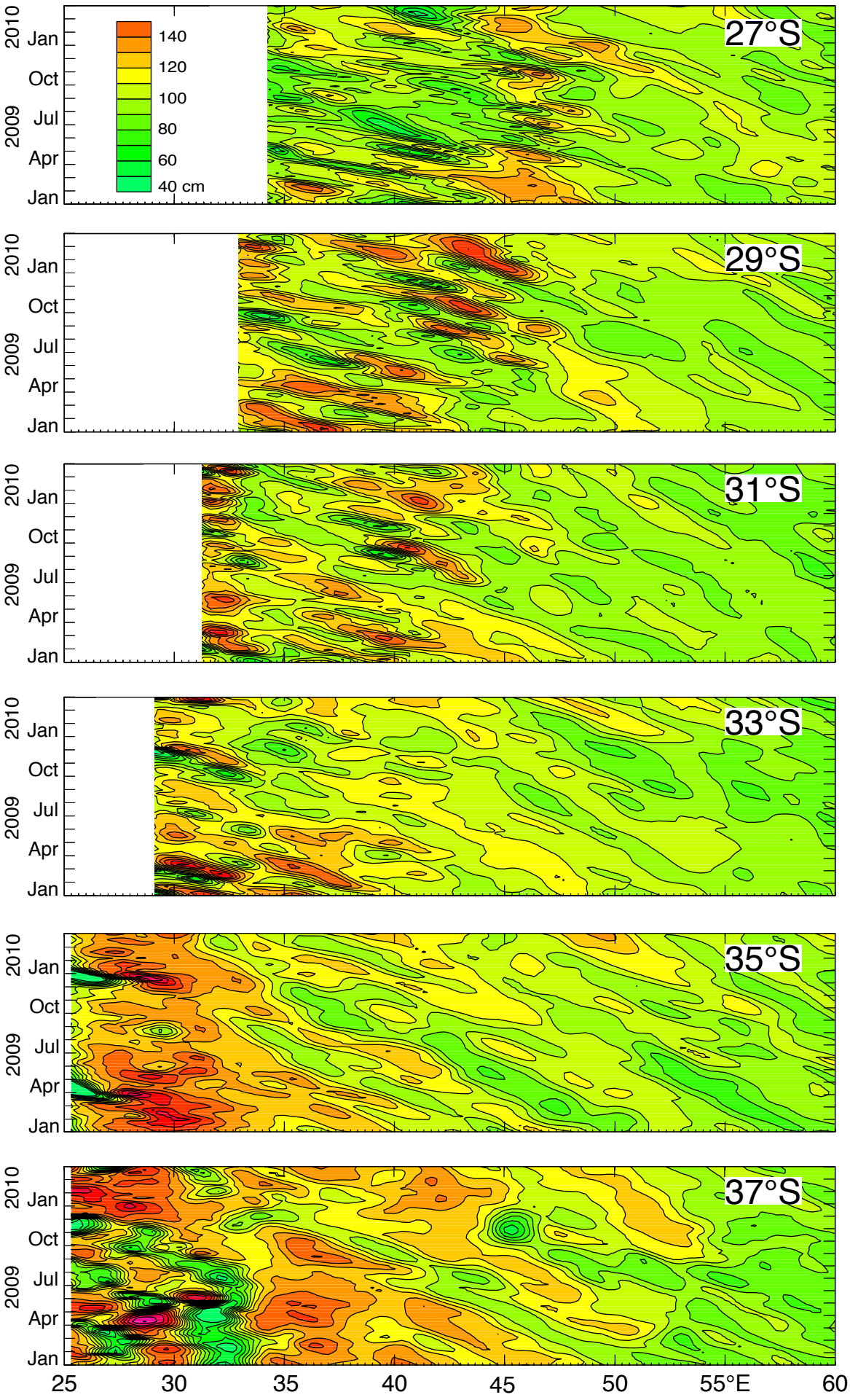

Fig. 4 Hovmöller plots of AVISO sea surface height against longitude and time show westward propagation of features at all latitudes between Madagascar and the ARC. Westward propagation ceases only close to the Agulhas and in the vicinity of the Agulhas retroflection.

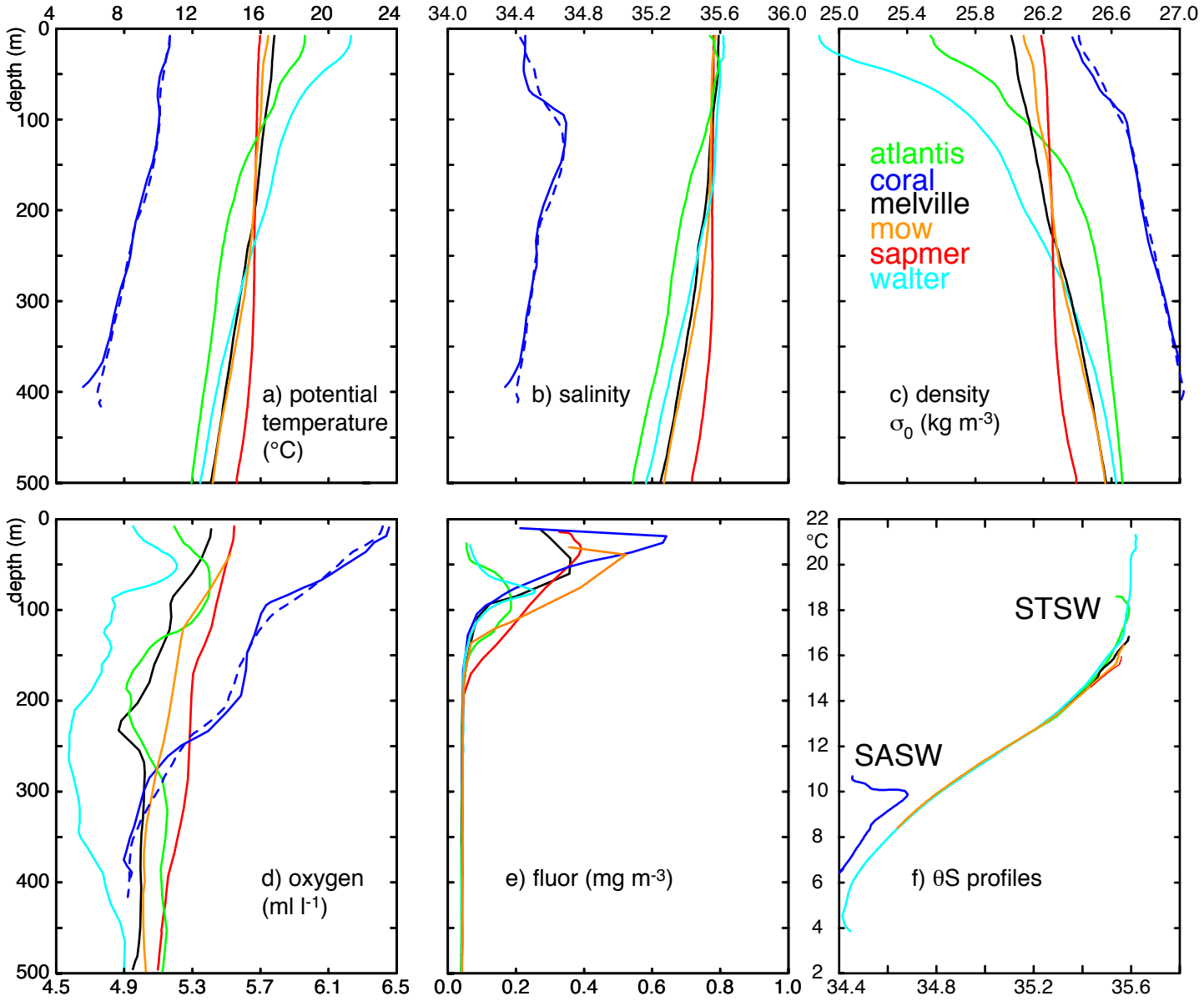

Fig. 5 Profiles of (a) potential temperature, (b) salinity, (c) density, (d) oxygen, (e) fluorescence against depth and (f) potential temperature against salinity at each seamount, averaged over 24 hours. Averages of properties including depth were calculated on density surfaces then plotted against the averaged depth, in order to avoid smoothing of features which can result from normal depth averaging. The most pronounced differences were at Coral (blue) where the depth averaged profiles are shown dashed for comparison. Depth averaging is more reliable near the surface and bottom of each profiles. Oxygen and fluorescence are not absolutely calibrated, for lack of calibration data, but depth dependent features are of interest. Subtropical Surface Water (STSW) and Subantarctic Surface Water (SASW) are marked on (f).